

Effect of laser spectral bandwidth on coherent control of resonance-enhanced multiphoton-ionization photoelectron spectroscopy

Shuwu Xu, Jingxin Ding, Chenhui Lu, Tianqing Jia, Shian Zhang, and Zhenrong Sun

Citation: *The Journal of Chemical Physics* **140**, 084312 (2014); doi: 10.1063/1.4866452

View online: <http://dx.doi.org/10.1063/1.4866452>

View Table of Contents: <http://scitation.aip.org/content/aip/journal/jcp/140/8?ver=pdfcov>

Published by the [AIP Publishing](#)



Re-register for Table of Content Alerts

Create a profile.



Sign up today!



Effect of laser spectral bandwidth on coherent control of resonance-enhanced multiphoton-ionization photoelectron spectroscopy

Shuwu Xu,^{1,2} Jingxin Ding,^{1,a)} Chenhui Lu,¹ Tianqing Jia,¹ Shian Zhang,^{1,b)} and Zhenrong Sun¹

¹State Key Laboratory of Precision Spectroscopy, and Department of Physics, East China Normal University, Shanghai 200062, People's Republic of China

²School of Science, Nantong University, Nantong 226007, People's Republic of China

(Received 3 November 2013; accepted 10 February 2014; published online 27 February 2014)

The high-resolution (2 + 1) resonance-enhanced multiphoton-ionization photoelectron spectroscopy (REMPI-PS) can be obtained by measuring the photoelectron intensity at a given kinetic energy and scanning the single π phase step position. In this paper, we further demonstrate that the high-resolution (2 + 1) REMPI-PS cannot be achieved at any measured position of the kinetic energy by this measurement method, which is affected by the laser spectral bandwidth. We propose a double π phase step modulation to eliminate the effect of the laser spectral bandwidth, and show the advantage of the double π phase step modulation on achieving the high-resolution (2 + 1) REMPI-PS by considering the contributions involving on- and near-resonant three-photon excitation pathways. © 2014 AIP Publishing LLC. [<http://dx.doi.org/10.1063/1.4866452>]

Recently, resonance-enhanced multiphoton-ionization photoelectron spectroscopy (REMPI-PS) has shown to be an effective method to study the energy-level structure of the excited or Rydberg state and the photoionization or photodissociation processes.^{1–8} Femtosecond laser pulse was considered as an ideal excitation source because of its ultrahigh laser intensity and ultrashort pulse duration. However, the femtosecond-induced REMPI-PS suffers from poor spectral resolution due to the large spectral width of the femtosecond laser pulse, and this greatly limits its further applications and developments. Therefore, a crucial question for the femtosecond-induced REMPI-PS is how to improve its spectral resolution. Fortunately, with the advent of the ultrafast pulse shaping technique,^{9–14} the quantum coherent control strategy by making use of the shaped femtosecond laser pulse provides a new opportunity to manipulate the resonance-enhanced multiphoton ionization process via the quantum interference of different excitation pathways connecting the initial state and the desired final state. Nowadays, the femtosecond pulse shaping technique has proven to be a well-established tool to improve the spectral resolution of the femtosecond-induced REMPI-PS. For example, Wollenhaupt *et al.* demonstrated that the slow and fast photoelectron components of the femtosecond-induced REMPI-PS can be selectively excited by a sinusoidal, chirped, or phase-step modulation.^{15–18} We showed that the femtosecond-induced REMPI-PS can be greatly narrowed and enhanced by a π or cubic phase modulation.^{19–23}

In our previous study,²³ we demonstrated that, by measuring the photoelectron intensity at a given kinetic energy and scanning the single π phase step position, a high-resolution (2 + 1) REMPI-PS can be obtained. However, in present study we will demonstrate that the high-resolution

(2 + 1) REMPI-PS cannot be achieved at any measured position of the kinetic energy by this measurement method, which is dependent of the laser spectral bandwidth. To eliminate the effect of the laser spectral bandwidth, we propose a double π phase step modulation instead of the single π phase step modulation, and show that the high-resolution (2 + 1) REMPI-PS can be realized at any measured position of the kinetic energy and with any laser spectral bandwidth. Furthermore, to show the advantage of the double π phase step modulation, we utilize the contributions involving the on- and near-resonant three-photon excitation processes to illustrate the control of the photoelectron intensity.

Figure 1(a) presents the schematic diagram of the (2 + 1) resonance-enhanced three-photon ionization process in cesium (Cs) atom pumped by the femtosecond laser field $E(t)$, where $|6s\rangle$ and $|9s\rangle$ are the ground state and the excited state, respectively. The state transition $|6s\rangle \rightarrow |9s\rangle$ is coupled by a non-resonant two-photon absorption, and then the population in the $|9s\rangle$ state is ionized by absorbing the other photon. In perturbative regime, the (2 + 1) REMPI-PS signal $P^{(2+1)}(E_v)$ can be approximated by time-dependent perturbation theory as²³

$$P^{(2+1)}(E_v) \propto |A_{on-res}^{(2+1)}(E_v) + A_{near-res}^{(2+1)}(E_v)|^2, \quad (1)$$

where $A_{on-res}^{(2+1)}(E_v)$ and $A_{near-res}^{(2+1)}(E_v)$ represent, respectively, the on- and near-resonant components, and are given by

$$A_{on-res}^{(2+1)}(E_v) = i\pi E[(E_v + E_I)/\hbar - \omega_{6s \rightarrow 9s}]S^{(2)}(\omega_{6s \rightarrow 9s}) \quad (2)$$

and

$$A_{near-res}^{(2+1)}(E_v) = -\wp \int_{-\infty}^{+\infty} (1/\Delta) E \times [(E_v + E_I)/\hbar - \omega_{6s \rightarrow 9s} - \Delta] \times S^{(2)}(\omega_{6s \rightarrow 9s} + \Delta) d\Delta, \quad (3)$$

^{a)}Email: jxding@phy.ecnu.edu.cn

^{b)}Email: sazhang@phy.ecnu.edu.cn

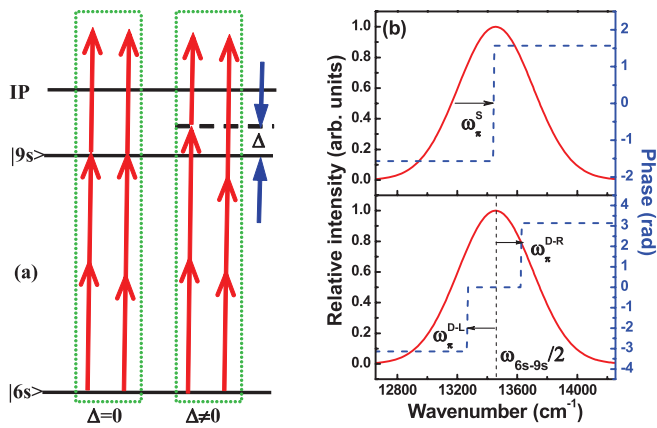


FIG. 1. (a) The $(2+1)$ resonance-enhanced three-photon ionization process in Cs atom with different excitation pathways that are on-resonance ($\Delta = 0$) or near-resonance ($\Delta \neq 0$) with the excited state $|9s\rangle$. (b) The femtosecond laser spectrum modulated by two types of spectral phase patterns with the single π phase step modulation (upper panel) and the double π phase step modulation (lower panel).

with

$$S^{(2)}(\Omega) = \int_{-\infty}^{+\infty} E(\omega) E(\Omega - \omega) d\omega, \quad (4)$$

where E_I is the ionization energy from the $|6s\rangle$ state, $\omega_{6s \rightarrow 9s}$ is the transition frequency from the states $|6s\rangle$ to $|9s\rangle$, \wp is the Cauchy's principal-value operator, Δ is the detuning of the non-resonant two-photon absorption in the $|9s\rangle$ state, and $E(\omega)$ is Fourier transform of $E(t)$ with $E(\omega) = A(\omega)\exp[i\Phi(\omega)]$, here $A(\omega)$ and $\Phi(\omega)$ are the spectral amplitude and phase in the frequency domain, respectively. One can see from Eqs. (2) and (3) that the on-resonant term $A_{\text{on-res}}^{(2+1)}(E_v)$ interferes all on-resonant three-photon excitation pathways ($\Delta = 0$) while the near-resonant term $A_{\text{near-res}}^{(2+1)}(E_v)$ interferes all other near-resonant three-photon excitation pathways ($\Delta \neq 0$), and therefore the total signal $P^{(2+1)}(E_v)$ is the result of both the inter- and intra-group interferences involving the on- and near-resonant three-photon excitation pathways.

As can be seen from Eqs. (2)–(4), the on-resonant term $A_{\text{on-res}}^{(2+1)}(E_v)$ is proportional to the non-resonant two-photon absorption amplitude $S^{(2)}(\omega_{6s \rightarrow 9s})$ and therefore is maximal value for the transform-limited laser pulse or the shaped laser pulse with antisymmetric spectral phase distribution around the two-photon transition frequency $\omega_{6s \rightarrow 9s}/2$. Thus, the on-resonant contribution $|A_{\text{on-res}}^{(2+1)}(E_v)|^2$ can be suppressed but cannot be enhanced by varying the laser spectral phase. However, the near-resonant term $A_{\text{near-res}}^{(2+1)}(E_v)$ integrates over both positive ($\Delta > 0$) and negative ($\Delta < 0$) components, and therefore the transform-limited laser pulse induces a destructive interference in these near-resonant three-photon excitation pathways. A simple way to enhance the near-resonant contribution $|A_{\text{near-res}}^{(2+1)}(E_v)|^2$ is to induce a constructive interference instead of the destructive interference by a phase inversion, such as the spectral phase step modulation that we will demonstrate in this paper.

In our theoretical simulation, the transition frequency from the states $|6s\rangle$ to $|9s\rangle$ in Cs atom is $\omega_{6s \rightarrow 9s}$

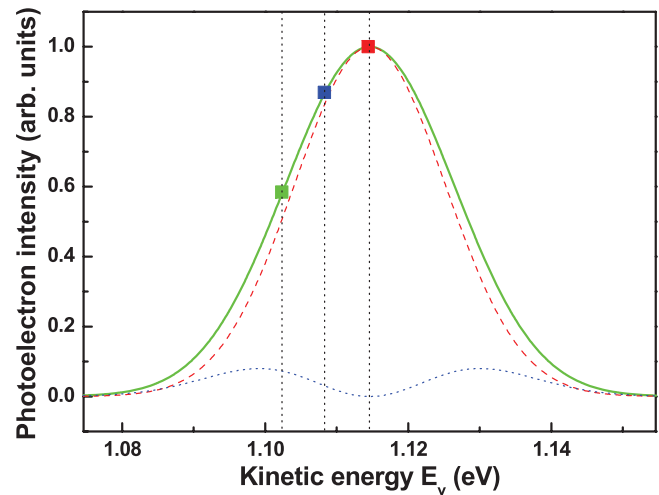


FIG. 2. The normalized REMPI-PS signal $P^{(2+1)}(E_v)$ (green solid line) induced by the transform-limited laser pulse, together with the on-resonant contribution $|A_{\text{on-res}}^{(2+1)}(E_v)|^2$ (red dashed lines) and near-resonant contribution $|A_{\text{near-res}}^{(2+1)}(E_v)|^2$ (blue dotted lines), and the three vertical dashed lines are used to indicate the measured positions of the kinetic energy.

$= 26910 \text{ cm}^{-1}$, the ionization energy from the $|6s\rangle$ state is $E_I = 3.89 \text{ eV}$, which is corresponding to the frequency of about 31375 cm^{-1} , and the central frequency of the femtosecond laser pulse is set to be $\omega_L = \omega_{6s \rightarrow 9s}/2 = 13455 \text{ cm}^{-1}$. Figure 2 presents the REMPI-PS signal $P^{(2+1)}(E_v)$ (green solid line) excited by the transform-limited laser pulse, and the on-resonant contribution $|A_{\text{on-res}}^{(2+1)}(E_v)|^2$ (red dashed lines) and near-resonant contribution $|A_{\text{near-res}}^{(2+1)}(E_v)|^2$ (blue dotted lines) are also shown together. All traces are normalized by the maximal photoelectron intensity. One can see that, under the excitation of the transform-limited laser pulse, the resonance-mediated three-photon excitation process is dominated by the on-resonant contribution $|A_{\text{on-res}}^{(2+1)}(E_v)|^2$, while the near-resonant contribution $|A_{\text{near-res}}^{(2+1)}(E_v)|^2$ is very small. Our previous works showed that, by measuring the photoelectron intensity at a given kinetic energy and scanning the single π phase step position, the high-resolution $(2+1)$ REMPI-PS can be obtained.²³ In order to show that the high-resolution photoelectron spectroscopy will be affected by the laser spectral bandwidth, we measure three different positions of the kinetic energy that are at $E_v^{\text{meas}} = 1.1022, 1.1084, \text{ and } 1.1146 \text{ eV}$, as shown with three vertical dashed lines in Fig. 2.

Figure 3 presents the normalized photoelectron intensities $P^{(2+1)}(E_v^{\text{meas}})$ (green solid lines) measured at the kinetic energies $E_v^{\text{meas}} = 1.1146$ (a), 1.1084 (b), and 1.1022 eV (c) as the function of the single π phase step position ω_π^S with the laser spectral bandwidths $\Delta\omega = 100$ (left panels), 200 (middle panels), and 300 cm^{-1} (right panels), together with the on-resonant contribution $|A_{\text{on-res}}^{(2+1)}(E_v^{\text{meas}})|^2$ (red dashed lines) and near-resonant contribution $|A_{\text{near-res}}^{(2+1)}(E_v^{\text{meas}})|^2$ (blue dotted lines). The single π phase step modulation is shown in the upper panel of Fig. 1(b), where the phase pattern is characterized by a phase jump from $-\pi/2$ to $\pi/2$ at the variable step position ω_π^S . All data are normalized by the photoelectron intensity induced by the transform-limited laser pulse, and hereafter the same method is employed. As shown in Fig. 3(a),

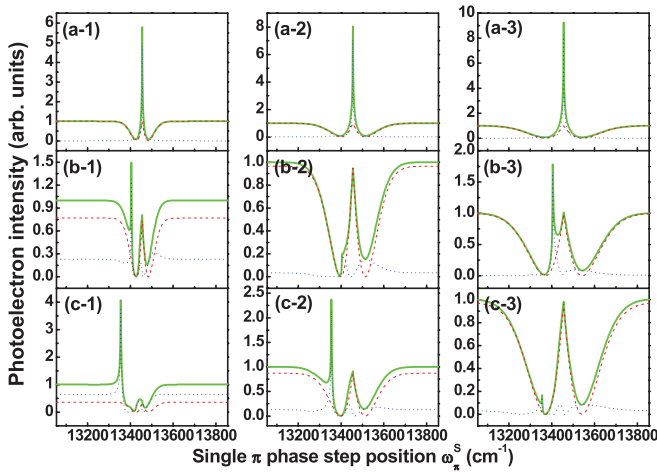


FIG. 3. The normalized photoelectron intensities $P^{(2+1)}(E_v^{\text{meas}})$ (green solid lines) measured at the kinetic energies $E_v^{\text{meas}} = 1.1146$ (a), 1.1084 (b), and 1.1022 eV (c) as the function of the single π phase step position ω_π^S with the laser spectral bandwidths $\Delta\omega = 100$ (left panels), 200 (middle panels), and 300 cm^{-1} (right panels), and also the on-resonant contribution $|A_{\text{on-res}}^{(2+1)}(E_v^{\text{meas}})|^2$ (red dashed lines) and near-resonant contribution $|A_{\text{near-res}}^{(2+1)}(E_v^{\text{meas}})|^2$ (blue dotted lines) are presented.

when the measured position of the kinetic energy is at $E_v^{\text{meas}} = 1.1146$ eV, corresponding to the maximal photoelectron intensity, one narrowband peak at the step position $\omega_\pi^S = 13455$ cm^{-1} can be observed with any laser spectral bandwidth, that is to say, in this case the high-resolution photoelectron spectroscopy is not correlated with the laser spectral bandwidth. However, different results can be found when the measured positions of the kinetic energy are not corresponding to the maximal photoelectron intensity, as shown in Figs. 3(b) and 3(c), where the measured positions of the kinetic energy are at $E_v^{\text{meas}} = 1.1084$ and 1.1022 eV, respectively. One can see from Fig. 3(b) that the narrowband peak at the step position $\omega_\pi^S = 13405$ cm^{-1} can be achieved with the laser spectral bandwidths $\Delta\omega = 100$ and 300 cm^{-1} (see Figs. 3(b-1) and 3(b-3)), while it will be almost eliminated with the laser spectral bandwidth $\Delta\omega = 200$ cm^{-1} (see Fig. 3(b-2)). The similar results can be observed in Fig. 3(c), where the narrowband peak almost disappears with the laser spectral bandwidth $\Delta\omega = 300$ cm^{-1} (see Fig. 3(c-3)). Obviously, by the single π phase step modulation, the high-resolution REMPI-PS cannot be obtained at any given measured position of the kinetic energy, which is affected by the laser spectral bandwidth. By further observing the on-resonant contribution $|A_{\text{on-res}}^{(2+1)}(E_v^{\text{meas}})|^2$ and near-resonant contribution $|A_{\text{near-res}}^{(2+1)}(E_v^{\text{meas}})|^2$, the essential reason for the disappearance of the narrowband peaks in Figs. 3(b-2) and 3(c-3) is that the near-resonant contribution $|A_{\text{near-res}}^{(2+1)}(E_v^{\text{meas}})|^2$ at these π phase step positions is not large enough to far exceed the on-resonant contribution $|A_{\text{on-res}}^{(2+1)}(E_v^{\text{meas}})|^2$.

In order to eliminate the effect of the laser spectral bandwidth mentioned above, we proposed a double π phase step modulation instead of the single π phase step modulation, as shown in the lower panel of Fig. 1(b). The phase distribution is composed of two equal π phase steps with the left step $\omega_\pi^{\text{D-L}}$ from $-\pi$ to 0 and the right step $\omega_\pi^{\text{D-R}}$ from 0 to π , and the two phase steps are symmetrically

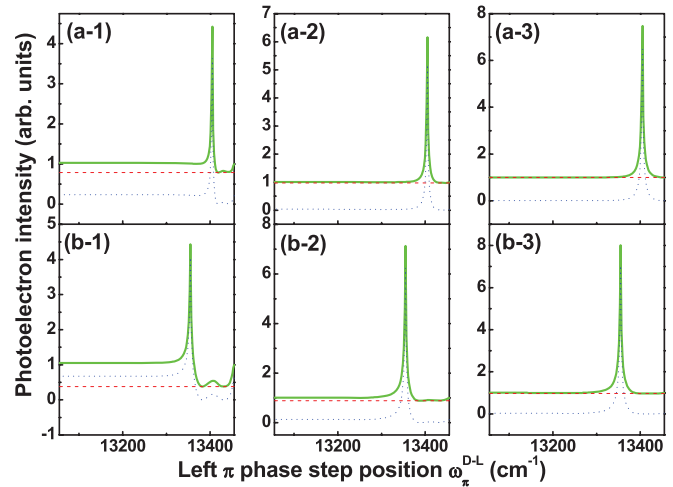


FIG. 4. The normalized photoelectron intensities $P^{(2+1)}(E_v^{\text{meas}})$ (green solid lines) measured at the kinetic energies $E_v^{\text{meas}} = 1.1084$ (a) and 1.1022 eV (b) as the function of the left π phase step position $\omega_\pi^{\text{D-L}}$ with the laser spectral bandwidths $\Delta\omega = 100$ (left panels), 200 (middle panels) and 300 cm^{-1} (right panels), and the on-resonant contribution $|A_{\text{on-res}}^{(2+1)}(E_v^{\text{meas}})|^2$ (red dashed lines) and near-resonant contribution $|A_{\text{near-res}}^{(2+1)}(E_v^{\text{meas}})|^2$ (blue dotted lines) are also shown.

positioned at the two-photon transition frequency $\omega_{6s \rightarrow 9s}/2$. Figure 4 presents the normalized photoelectron intensities $P^{(2+1)}(E_v^{\text{meas}})$ (green solid lines) measured at the kinetic energies $E_v^{\text{meas}} = 1.1084$ (a) and 1.1022 eV (b) as the function of the left π phase step position $\omega_\pi^{\text{D-L}}$ with the laser spectral bandwidths $\Delta\omega = 100$ (left panels), 200 (middle panels), and 300 cm^{-1} (right panels), and also the on-resonant contribution $|A_{\text{on-res}}^{(2+1)}(E_v^{\text{meas}})|^2$ (red dashed lines) and near-resonant contribution $|A_{\text{near-res}}^{(2+1)}(E_v^{\text{meas}})|^2$ (blue dotted lines) are given. As can be seen, these narrowband peaks at the left π phase step positions $\omega_\pi^{\text{D-L}} = 13405$ cm^{-1} and 13355 cm^{-1} always can be observed for any laser spectral bandwidth. In other words, by the double π phase step modulation, the high-resolution REMPI-PS can be obtained at any measured position of the kinetic energy, which is independent of the laser spectral bandwidth. Similarly, by observing the on-resonant contribution $|A_{\text{on-res}}^{(2+1)}(E_v^{\text{meas}})|^2$ and near-resonant contribution $|A_{\text{near-res}}^{(2+1)}(E_v^{\text{meas}})|^2$, the on-resonant contribution $|A_{\text{on-res}}^{(2+1)}(E_v^{\text{meas}})|^2$ is a constant due to the antisymmetric spectral phase distribution, while the near-resonant contribution $|A_{\text{near-res}}^{(2+1)}(E_v^{\text{meas}})|^2$ are greatly enhanced at these specific phase step positions due to the constructive interference instead of the destructive interference, and therefore the total signal $P^{(2+1)}(E_v^{\text{meas}})$ is enhanced at these corresponding positions.

To further show why the double π phase step modulation is more effective than the single π phase step modulation in obtaining the high-resolution REMPI-PS for any measured position of the kinetic energy and any laser spectral bandwidth, we present the dependence of the photoelectron intensities at the kinetic energies $E_v^{\text{meas}} = 1.1084$ and 1.1022 eV on the laser spectral bandwidth by both the single and double π phase step modulations, and the calculated results are presented in Fig. 5. By the single π phase step modulation, as shown in Fig. 5(a-1), both the on-resonant contribution $|A_{\text{on-res}}^{(2+1)}(E_v^{\text{meas}})|^2$ and near-resonant

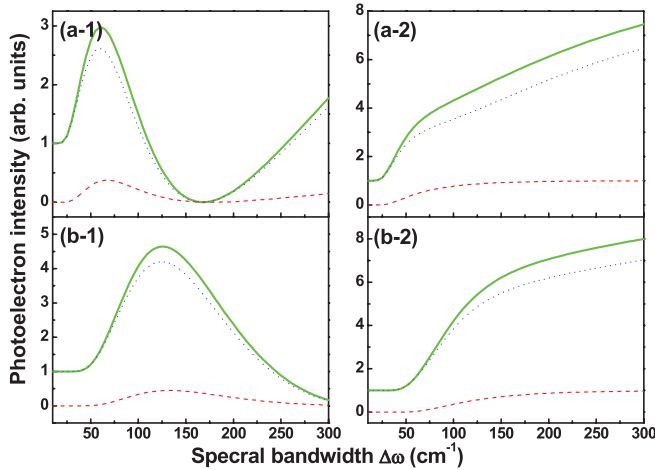


FIG. 5. The normalized photoelectron intensities $P^{(2+1)}(E_v^{\text{meas}})$ (green solid lines) measured at the kinetic energies $E_v^{\text{meas}} = 1.1084$ (a) and 1.1022 eV (b) as the function of the laser spectral bandwidth $\Delta\omega$ with the single π phase step positions $\omega_\pi^S = 13405$ (a-1) and 13355 cm^{-1} (b-1) and the left π phase step positions $\omega_\pi^{D-L} = 13405$ (a-2) and 13355 cm^{-1} (b-2), and the on-resonant contribution $|A_{\text{on-res}}^{(2+1)}(E_v^{\text{meas}})|^2$ (red dashed lines) and near-resonant contribution $|A_{\text{near-res}}^{(2+1)}(E_v^{\text{meas}})|^2$ (blue dotted lines) are also given.

contribution $|A_{\text{near-res}}^{(2+1)}(E_v^{\text{meas}})|^2$ are completely suppressed with the laser spectral bandwidth $\Delta\omega = 170$ cm^{-1} and therefore the total signal $P^{(2+1)}(E_v^{\text{meas}})$. The similar results can also be found in Fig. 5(b-1) around the laser spectral bandwidth $\Delta\omega = 300$ cm^{-1} . Thus, the narrowband peak by scanning the single π phase step position will disappear with these specific laser spectral bandwidths, as shown in Figs. 3(b-2) and 3(c-3). However, by the double π phase step modulation, as shown in Figs. 5(a-2) and 5(b-2), the near-resonant contribution $|A_{\text{near-res}}^{(2+1)}(E_v^{\text{meas}})|^2$ can be obviously enhanced with any laser spectral bandwidth and is far larger than the on-resonant contribution $|A_{\text{on-res}}^{(2+1)}(E_v^{\text{meas}})|^2$, and therefore the total signal $P^{(2+1)}(E_v^{\text{meas}})$ is greatly enhanced. Consequently, the narrowband peak by scanning the double π phase step position always can be obtained with any laser spectral bandwidth, as shown in Fig. 4.

The effects of the laser spectral bandwidth on the photoelectron intensity at a given kinetic energy by the single and double π phase step modulations in Figs. 3–5 can be analyzed by the theoretical description formulated in Eqs. (2)–(4). The single or double π phase step modulation (i.e., $\Phi(\omega) = 0$ or π) implies that the shaped laser field $E(\omega)$ is always a positive or negative real number for any laser frequency, and thus the on-resonant component $A_{\text{on-res}}^{(2+1)}(E_v^{\text{meas}})$ is imaginary number while the near-resonant component $A_{\text{near-res}}^{(2+1)}(E_v^{\text{meas}})$ is real number. In this case, the photoelectron intensity $P^{(2+1)}(E_v^{\text{meas}})$ is the sum of the on-resonant contribution $|A_{\text{on-res}}^{(2+1)}(E_v^{\text{meas}})|^2$ and near-resonant contribution $|A_{\text{near-res}}^{(2+1)}(E_v^{\text{meas}})|^2$, i.e., $P^{(2+1)}(E_v^{\text{meas}}) = |A_{\text{on-res}}^{(2+1)}(E_v^{\text{meas}})|^2 + |A_{\text{near-res}}^{(2+1)}(E_v^{\text{meas}})|^2$. In other words, the $(2 + 1)$ resonance-enhanced three-photon ionization is determined only by intra-group interferences within each of the on- and near-resonant excitation pathways. By the single π phase step modulation, the amplitudes $(1/\Delta)E[(E_v^{\text{meas}} + E_I)/\hbar - \omega_{6s \rightarrow 9s} - \Delta]$ are all negative value for small $+\Delta$ and $-\Delta$ with any laser

spectral bandwidth while the amplitudes $S^{(2)}(\omega_{6s \rightarrow 9s} + \Delta)$ will change from positive to negative value with the increase of the laser spectral bandwidth,²⁴ and thus the negatively and positively detuned near-resonant three-photon excitation pathways will constructively (or destructively) interfere when the amplitudes $S^{(2)}(\omega_{6s \rightarrow 9s} + \Delta)$ are of the same (or different) sign. Consequently, both the on-resonant contribution $|A_{\text{on-res}}^{(2+1)}(E_v^{\text{meas}})|^2$ and near-resonant contribution $|A_{\text{near-res}}^{(2+1)}(E_v^{\text{meas}})|^2$ will be suppressed at some specific laser spectral bandwidths and therefore photoelectron intensity $P^{(2+1)}(E_v^{\text{meas}})$, as shown in Figs. 3 and 5(a). By the double π phase step modulation, the amplitudes $(1/\Delta)E[(E_v^{\text{meas}} + E_I)/\hbar - \omega_{6s \rightarrow 9s} - \Delta]$ have the same sign for small $\pm|\Delta|$ with any laser spectral bandwidth and the amplitudes $S^{(2)}(\omega_{6s \rightarrow 9s} + \Delta)$ are all positive value,²⁴ and therefore the interferences between negatively and positively detuned near-resonant three-photon excitation pathways are constructive. Thus, the near-resonant contribution $|A_{\text{near-res}}^{(2+1)}(E_v^{\text{meas}})|^2$ can be enhanced for any laser spectral bandwidth and the on-resonant contribution $|A_{\text{on-res}}^{(2+1)}(E_v^{\text{meas}})|^2$ keeps its maximal value due to the antisymmetric spectral phase distribution, and therefore the photoelectron intensity $P^{(2+1)}(E_v^{\text{meas}})$ always can be enhanced, as shown in Figs. 4 and 5(b).

In conclusion, we have demonstrated that the laser spectral bandwidth will affect the high-resolution $(2 + 1)$ REMPI-PS by measuring the photoelectron intensity at a given kinetic energy and scanning the single π phase step modulation, and a double π phase step modulation instead of the single π phase step modulation was proposed to eliminate the effect of the laser spectral bandwidth, thus the high-resolution $(2 + 1)$ REMPI-PS can be achieved at any measured position of the kinetic energy and with any laser spectral bandwidth. By considering the contributions involving on- and near-resonant three-photon excitation processes, the advantage of the double π phase step modulation on achieving the high-resolution $(2 + 1)$ REMPI-PS can be well illustrated. We believe that these theoretical results are very helpful for the experimental study and can be further extended to the control of various resonance-enhanced multiphoton-ionization processes.

This work was partly supported by National Natural Science Fund (Grant Nos. 11004060, 11027403, and 51132004) and Shanghai Rising-Star Program (Grant No. 12QA1400900).

- ¹J. Wassaf, V. Vénierd, R. Taïeb, and A. Maquet, *Phys. Rev. Lett.* **90**, 013003 (2003).
- ²S. Zhang, J. Zhu, C. Lu, T. Jia, J. Qiu, and Z. Sun, *RSC Adv.* **3**, 12185 (2013).
- ³T. A. Barckholtz, D. E. Powers, T. A. Miller, and B. E. Bursten, *J. Am. Chem. Soc.* **121**, 2576 (1999).
- ⁴X. K. Hu, J. B. A. Mitchell, and R. H. Lipson, *Phys. Rev. A* **62**, 052712 (2000).
- ⁵M. Wollenhaupt, V. Engle, and T. Baumert, *Annu. Rev. Phys. Chem.* **56**, 25 (2005).
- ⁶H. Liu, S. Yin, J. Zhang, L. Wang, B. Jiang, and N. Lou, *Phys. Rev. A* **74**, 053418 (2006).
- ⁷Y. Hikosaka, M. Fushitani, A. Matsuda, C. M. Tseng, A. Hishikawa, E. Shigemasa, M. Nagasono, K. Tono, T. Togashi, H. Ohashi, H. Kimura, Y. Senba, M. Yabashi, and T. Ishikawa, *Phys. Rev. Lett.* **105**, 133001 (2010).
- ⁸J. Zhang, C. Harthcock, F. Y. Han, and W. Kong, *J. Chem. Phys.* **135**, 244306 (2011).

- ⁹A. M. Weiner, *Rev. Sci. Instrum.* **71**, 1929 (2000).
- ¹⁰C. Brif, R. Chakrabarti, and H. Rabitz, *New J. Phys.* **12**, 075008 (2010).
- ¹¹Y. Silberberg, *Annu. Rev. Phys. Chem.* **60**, 277 (2009).
- ¹²P. Nuernberger, G. Nogt, T. Brixner, and G. Gerber, *Phys. Chem. Chem. Phys.* **9**, 2470 (2007).
- ¹³D. Goswami, *Phys. Rep.* **374**, 385 (2003).
- ¹⁴F. Gao, F. Shuang, J. Shi, H. Rabitz, H. Wang, and J. Cheng, *J. Chem. Phys.* **136**, 144114 (2012).
- ¹⁵M. Wollenhaupt, A. Prækelt, C. Sarpe-Tudoran, D. Liese, T. Bayer, and T. Baumert, *Phys. Rev. A* **73**, 063409 (2006).
- ¹⁶M. Wollenhaupt, A. Prækelt, C. Sarpe-Tudoran, D. Liese, T. Bayer, and T. Baumert, *Appl. Phys. B* **82**, 183 (2006).
- ¹⁷T. Bayer, M. Wollenhaupt, C. Sarpe-Tudoran, and T. Baumert, *Phys. Rev. Lett.* **102**, 0230041 (2009).
- ¹⁸M. Wollenhaupt, T. Bayer, N. V. Vitanov, and T. Baumert, *Phys. Rev. A* **81**, 053422 (2010).
- ¹⁹S. Zhang, H. Zhang, T. Jia, Z. Wang, and Z. Sun, *J. Phys. B* **43**, 135401 (2010).
- ²⁰S. Zhang, C. Lu, T. Jia, and Z. Sun, *Phys. Rev. A* **86**, 012513 (2012).
- ²¹S. Zhang, C. Lu, T. Jia, J. Qiu, and Z. Sun, *J. Chem. Phys.* **137**, 174301 (2012).
- ²²S. Zhang, C. Lu, T. Jia, J. Qiu, and Z. Sun, *Phys. Rev. A* **86**, 043433 (2012).
- ²³S. Zhang, C. Lu, T. Jia, J. Qiu, and Z. Sun, *Phys. Rev. A* **88**, 043437 (2013).
- ²⁴A. Gandman, L. Chuntunov, L. Rybak, and Z. Amity, *Phys. Rev. A* **76**, 053419 (2007).